PHYSICAL REVIEW B **79**, 195122 (2009)

Tetragonal CuO: End member of the 3*d* transition metal monoxides

Wolter Siemons,[1,2] Gertjan Koster,[1,2,*] Dave H. A. Blank,[1] Robert H. Hammond,[2]
Theodore H. Geballe,[2] and Malcolm R. Beasley[2]

[1]*Faculty of Science and Technology and MESA+Institute for Nanotechnology, University of Twente, 7500 AE Enschede, The Netherlands*
[2]*Geballe Laboratory for Advanced Materials, Stanford University, Stanford, California 94305, USA*

(Received 28 October 2008; revised manuscript received 25 February 2009; published 22 May 2009)

Monoclinic CuO is anomalous both structurally as well as electronically in the 3*d* transition metal oxide series. All the others have the cubic rocksalt structure. Here we report the synthesis and electronic property determination of a tetragonal (elongated rocksalt) form of CuO created using an epitaxial thin-film deposition approach. *In situ* photoelectron spectroscopy suggests an enhanced charge-transfer gap Δ with the overall bonding more ionic. As an end member of the 3*d* transition monoxides, its magnetic properties should be that of a high T_N antiferromagnet.

DOI: 10.1103/PhysRevB.79.195122 PACS number(s): 73.61.Le

I. INTRODUCTION

Since the discovery of high-temperature superconductivity in the copper oxide perovskites, its origin and mechanism are still unexplained and under debate. The original proposal by Bednorz and Mueller[1] and others that a Jahn-Teller distortion in a highly symmetric divalent copper monoxide structure introducing a strong electron-phonon interaction causes superconductivity has lead to extensive studies toward the synthesis of the family of cuprates. The simplest form, the cubic rocksalt copper monoxide, however, has not been found in nature nor has been successfully synthesized yet. CuO is the exceptional member of the rocksalt series as one traverses the periodic table from MnO to CuO. It deviates substantially from the trends exhibited by the members with lower atomic number. All the others have the cubic rocksalt structure and all are correlated antiferromagnetic (AFM) insulators.[2–5] CuO differs in having a monoclinic structure as opposed to the rocksalt structure of the other monoxides, and, as shown in Fig. 1, it also has a substantially lower Néel temperature than a simple extrapolation of the trend across the periodic table would suggest. Recently, ferroelectricity has been added to its list of properties.[6] Presumably, this exceptional behavior is a consequence of its lower-symmetry structure. Clearly, the properties of CuO in higher-symmetry structures would be of great fundamental interest in understanding correlated materials.[7,8] Here we report the synthesis and preliminary electronic property determination of a tetragonal [elongated rocksalt displayed in Fig. 1(b)] form of CuO created by using an epitaxial thin-film deposition approach. Looking ahead, if the trend shown in Fig. 1(a) was followed, the Néel temperature of rocksalt CuO would be very high (700–800 K), as would be its associated exchange coupling *J*. If such a high-*J* CuO could be doped, its properties would be of great interest in the context of the earlier mentioned high-T_c superconductors.

The films discussed in this work have been well characterized from the structural point of view using reflection

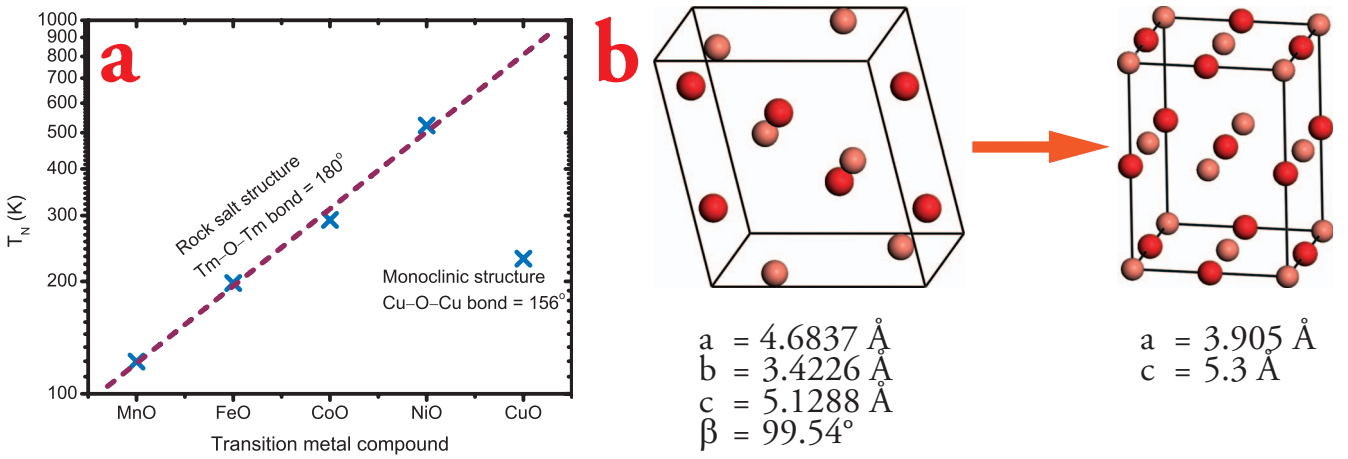

FIG. 1. (Color) (a) An overview of the Néel temperatures for transition metal monoxides with a rocksalt structure. T_N increases exponentially with each element up to NiO as indicated by the dashed line, which is a fit of the first four points. The T_N of the monoclinic CuO structure does not follow this trend, but is much lower, possibly due to a change in the Tm-O-Tm bond angle. When a rocksalt structure of CuO is formed, T_N might follow the trend and linear extrapolation predicts a T_N slightly higher than 800 K. (b) The change in unit-cell symmetry going from bulk (monoclinic) to the strained unit cell on $SrTiO_3$ (tetragonal), including the unit-cell parameters. The lighter colored atoms represent oxygen and the darker colored atoms represent copper.

high-energy electron-diffraction (RHEED) and x-ray photoemission diffraction (XPD), and from the electronic structure point of view using *in situ* x-ray and ultraviolet photoemission spectroscopy (PES) (XPS/UPS). As we will discuss below, by comparing with the stable copper oxides, we have determined that the Cu has a charge of +2 and that the tetragonal structure is more ionic than the monoclinic phase. Preliminary attempts to dope our films using charge transfer from overlayers have also been carried out. Taken together, the results demonstrate that higher-symmetry forms of this important correlated oxide are possible and available for physical study.

II. SYNTHESIS AND ANALYSIS

Our epitaxial films of tetragonal CuO were grown in a UHV chamber on $SrTiO_3$ substrates using pulsed laser deposition (PLD), although we have also grown samples using electron-beam evaporation. For PLD, a Lambda Physic LPX 210 KrF excimer laser produces a 248-nm-wavelength beam with a typical pulse length of 20–30 ns. A rectangular mask shapes the beam selecting only the homogeneous part, and a variable attenuator permits variation in the pulse energy. The variable attenuator also offers the possibility to run the laser at the same voltage every run, which ensures the same pulse shape every time and therefore the best reproducibility. A lens makes an image of the mask on the target resulting in a well-defined illuminated area. Energy density on the target was kept at 2.1 J cm^{-2} with a repetition rate of 1 Hz. The temperature of the substrate was fixed to 600 °C, higher than the optimal growth temperature of 400 °C for tenorite films found by Willmott *et al.*[9] Atomic oxygen was provided during deposition by a microwave plasma source (Astex SXRHA) with the source operating at 600 W with a flow of 2.5 SCCM oxygen, resulting in a background deposition pressure in the system of 1.5×10^{-5} Torr and an estimated 3×10^{17} oxygen atoms $cm^{-2}\,s^{-1}$.[10] The growth was monitored by RHEED.

Films were grown on either insulating or conducting (0.5% Nb doped) $SrTiO_3$. The latter offers the advantage of reduced charging when performing PES on the insulating CuO samples. Both types of substrates were TiO_2 terminated, as described by Koster *et al.*[11] In order to stabilize the new phase, it is of utmost importance to oxidize Cu to a 2 + state. This was accomplished by using a target of CuO and providing the atomic oxygen during deposition.

After deposition samples were cooled down in atomic oxygen. The films were typically unstable in atomic oxygen below 300 °C. Specifically, it was found that the films would relax to tenorite when cooled to room temperature under deposition conditions. To avoid this problem, the atomic oxygen was switched off at 300 °C and the sample then cooled to room temperature in molecular oxygen ($\sim10^{-5}$ Torr). These results imply that the stability line for the epitaxially stabilized tetragonal CuO when exposed to atomic oxygen lies around 300 °C.

The thickness of the tetragonal CuO samples is limited by a relaxation to the tenorite phase above a certain thickness. For most samples, 300 laser pulses were used in the PLD process to guarantee a streaky RHEED pattern with no three-dimensional (3D) spots. This corresponds to a layer thickness between 15 and 20 Å as determined with x-ray reflectivity and angle-resolved XPS measurements.[12] Atomic force microscopy (AFM) imaging confirms that thin samples are flat with the $SrTiO_3$ step structure still visible, whereas the samples that are thicker exhibit islands on top associated with the film growth process that cause the observed 3D RHEED pattern.

Let us note here that after exposure to air, the top layer of the CuO was found to degrade to tenorite, whereas the layer closest to the interface with $SrTiO_3$ is found to be mostly tetragonal. This result could be established using angle-dependent XPS, as discussed in detail in the thesis by Siemons.[13] Also, when a sample is kept under vacuum after growth, the CuO is slowly reduced over a period of days.[14] After four days, the intensity of the satellite peaks is reduced to about half their size after deposition. All XPS spectra are referenced with respect to the Ti 2*p* peak of the substrate.

The XPS and UPS measurements are performed *in situ* with a VG scientific ESCALAB Mark II system. The photon source for XPS is Al $K\alpha$ and for UPS measurements HeI (21.2 eV) radiation was used. Both sources are nonmonochromatic and spectra are corrected for satellites by use of software.

III. INITIAL GROWTH

When grown on doubly terminated substrates, the growth was found to be more 3D, and the films relaxed to the tenorite phase at an earlier stage in the deposition. Similar results were observed on other substrate materials, such as $DyScO_3$ and $LaAlO_3$, where 3D growth patterns of the relaxed structure would occur at a very early stage. Due to the polar nature of these materials, those substrates are either doubly terminated (a reliable method to make them singly terminated, such as with $SrTiO_3$ has not been fully developed) or complicates the layer-by-layer growth of a neutral material such as CuO.[15] In addition, these other substrates have different lattice parameters as well, which might affect their efficacy for epitaxy of CuO.

Figures 2(a)–2(c) show the evolution of the RHEED pattern in the case of successful growth of the tetragonal phase. Specifically, a streaky pattern, which is fourfold symmetric (Fig. 3) when the sample is rotated around the surface normal (see also below), emerges during deposition, without any 3D spots between the streaks. In contrast, Fig. 2(d) shows the RHEED pattern that emerges when the film relaxes to the tenorite phase. It is clearly different from that of the new tetragonal phase. Such a streaky pattern was observed before for the growth of CuO on MgO,[16] but no different symmetry of the CuO unit cell was observed in that work.

IV. DETERMINING LATTICE PARAMETERS

To determine the in-plane lattice parameters of the new phase, RHEED spectra were used. Spectra taken along the $SrTiO_3$ (10) and (11) are shown in Fig. 4. Note that the in-plane fourfold symmetry was verified by rotating the azi-

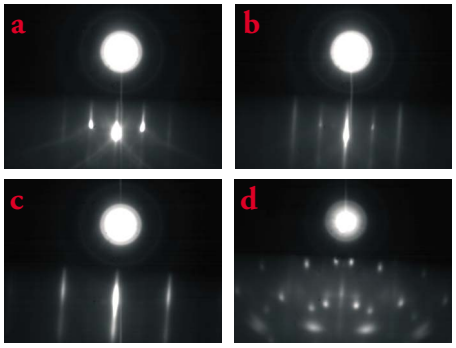

FIG. 2. (Color online) [(a)–(c)] The evolution of the RHEED spectrum during the growth of CuO on $SrTiO_3$ taken along the (01) direction of $SrTiO_3$ shows a transition from a clear 2D pattern for bare (a) $SrTiO_3$ to the streaky pattern of (c) CuO. (d) When growth is continued, the film relaxes to tenorite showing clear 3D spots.

muth of the sample, as shown in Fig. 3. Since the lattice parameters of the $SrTiO_3$ are well known (3.905 Å cubic), the lattice parameters of CuO can be calculated by comparing its lines to those of $SrTiO_3$. There is a subtlety here, however. One must correctly identify the lines. For a rocksalt structure, not all the diffraction peaks are allowed, and those that are allowed are different in two-dimensional (2D) and 3D. We find that for our very thin films, the 2D result is required. Specifically, in 2D the structure factor becomes

$$h,k \text{ unmixed: } F_{hk} = 2\sum_{n/2} f_n e^{2\pi i(hx_n+ky_n)},$$

$$h,k \text{ mixed: } F_{hk} = 0.$$

Therefore, in the 2D case, the (01) reflection is not allowed but the (11) is, and it follows that the shortest spacing between the RHEED lines corresponds to the (11) reflection. On the other hand, if the pattern were 3D, the shortest spacing would correspond to the (01) reflection. Analysis of the data assuming such an identification leads to nonphysical results.

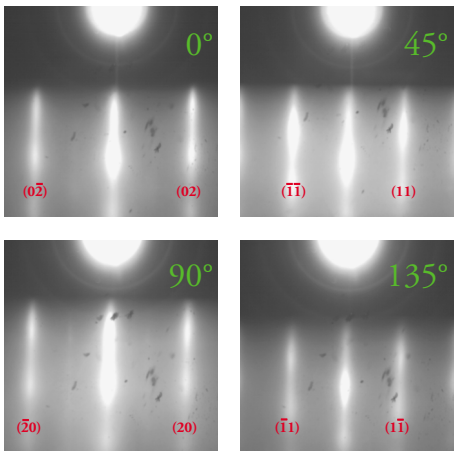

FIG. 3. (Color online) The electron-diffraction patterns of a tetragonal CuO film with the primary beam along its (10), (01), (1$\underline{1}$), (11) directions (0°, 90°, 45°, 135°, respectively). The patterns here show the in-plane fourfold symmetry when the sample is rotated around its azimuthal axis.

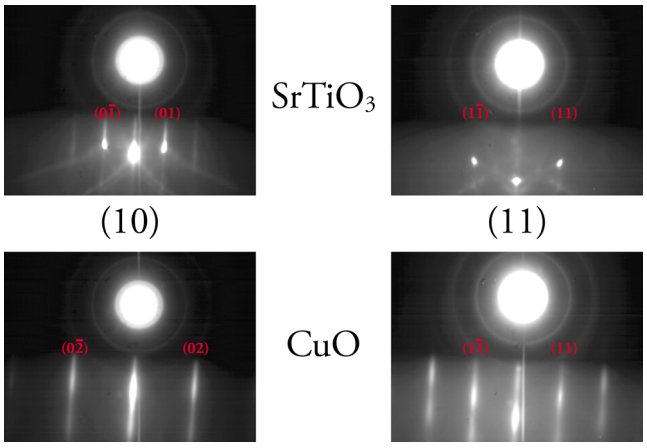

FIG. 4. (Color online) The electron-diffraction patterns of $SrTiO_3$ and CuO taken along their (10) and (11) directions. Even though the (10) reflection of CuO is not allowed as explained in the text, very faint lines at its position are usually visible.

With the dimensionality established, it is straightforward to determine the lattice constants (Fig. 4). In the (11) direction of the $SrTiO_3$ substrate, the (11) and (22) reflections of CuO are allowed, and along the (01) direction of the $SrTiO_3$, the (02) and (04) reflections of CuO are allowed. The CuO in-plane lattice parameters are exactly the same size as the $SrTiO_3$ underneath. This corresponds to a Cu-O bond length of 1.95 Å in plane, a number which corresponds well with values found in high-T_c materials or in monoclinic CuO. If the unit cell were cubic, this would result in a unit-cell volume of 59.5 Å, too far from the 81.1 $Å^3$ of tenorite to be physically reasonable. We conclude, therefore, that the unit cell must be elongated along the out-of-plane direction. But based on the RHEED spectra alone, we cannot draw conclusions about the out-of-plane lattice constant.

To measure the out-of-plane lattice constant, we employed XPD. To verify that the technique would produce reliable results, it was first applied to a conducting Nb-doped $SrTiO_3$ substrate. Simulations and measurements are strikingly similar. Two energies were measured: the O 1*s* and the Cu 2*p*. For the oxygen signal, a contribution of the substrate is to be expected since the escape depth of the electrons is on the order of the thickness of the CuO layer. The copper signal, on the other hand, comes solely from the film because the substrate contains no copper. We used the following procedure. The *c*-axis unit-cell parameter was changed in steps of 0.1 Å until the simulated spectrum matched the measurement. The degree of similarity was determined by looking at the most intense features first; the peaks that are caused by forward scattering. However, when these peaks are the same in simulation and measurement, the lower intensity data also show striking similarities. The resulting copper pattern shows a fourfold symmetry as shown on the right-hand side in Fig. 5, which is indicative of a fourfold symmetric unit cell, such as a rocksalt structure. By comparing simulations and measurements, the *c*-axis length of the unit cell was determined to be 5.3 Å. Using the XPD data, the out-of-

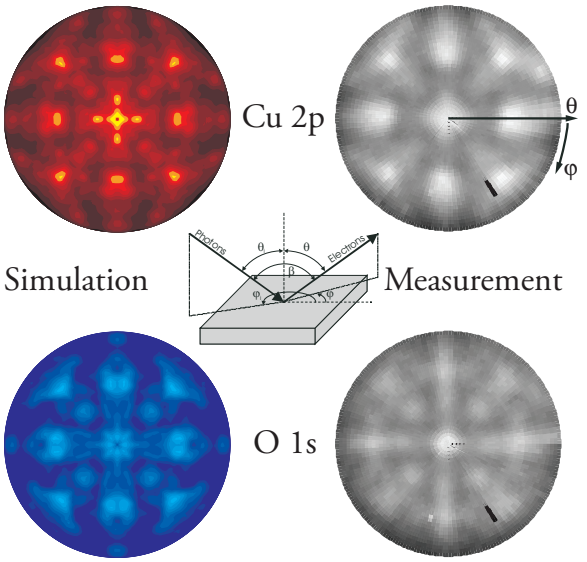

FIG. 5. (Color) XPD patterns for CuO measured (on the right) at two binding energies: the O 1*s* and the Cu $2p_{3/2}$ main line. The measurements were performed with the pass energy set at 100 eV, an acceptance angle of 5° in steps of 2° for θ (90–30°) and 3° for ϕ (0–360°). Simulations of the CuO in tetragonal form are shown on the left, as calculated with software by Abajo *et al.* (Ref. 17). The Cu signal comes solely from the film, whereas the O signal has a contribution from the substrate. The Cu pattern shows clear fourfold symmetry, which is not what would be expected from a single domain tenorite film.

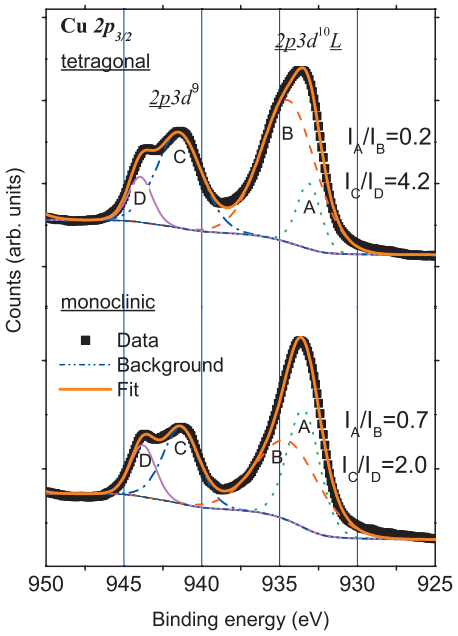

FIG. 6. (Color) The Cu 2*p* core-level XPS spectrum of the tetragonal CuO looks significantly different from the tenorite spectrum. Depicted are the Cu $2p_{3/2}$ peaks of the tetragonal (top) and monoclinic (bottom) phases. The data (squares) have been fitted using Guassian/Lorentian peak shapes and a Shirley background. The fit components are labeled *A* through *D* and the intensity ratios I_A/I_B and I_C/I_D are given as inset. After correction for He satellites contributions, the spectra have been normalized on the $2p_{1/2}$ peak (not shown) and the tenorite spectrum has been given an offset for clarity.

plane lattice parameter cannot be determined more accurately. These lattice parameters are also shown in Fig. 1(b). Note that the films described in this work typically are estimated to be 3 to 4 unit-cells thick.

With this complete set of unit-cell dimensions, the unit-cell volume now becomes 81.1 Å^3, which is the same as for tenorite and physically reasonable. The shortest Cu-O bond length in this structure is 1.95 Å, which corresponds to the value found in tenorite. The shortest Cu-Cu and O-O bond lengths are 2.76 Å, a value that is in between the values found for the two in tenorite.

V. ELECTRONIC STRUCTURE: RESULTS

Let us now turn to the electronic structure of this new phase of CuO. The XPS spectra of the Cu 2*p* lines for the thin tetragonal epitaxial films as well as those for thicker films, where the structure has relaxed to the tenorite structure, as observed by RHEED (see above) are shown in Fig. 6. The Cu $2p_{3/2}$ peak structure in both spectra is characteristic of copper containing compounds with a formal valence of 2, as is mostly revealed by the satellite structure. For tenorite, we find 934 eV for the binding energy of the Cu $2p_{3/2}$ main peak and 529.4 eV for the O 1*s* (not shown). These correspond well to the values found in literature, and with the additional observation that the oxygen peak is a single sharp line, we may conclude that the surface is mostly free of carbon-containing contaminants.[18–20] For the tetragonal phase, the energies of these lines do not appear to change significantly. There are significant differences though. Compared to the tenorite spectrum, the tetragonal CuO spectrum has a larger shoulder on the main peak at higher binding energy. Also, the symmetry as well as the spectral weight of the satellite peak has changed considerably. To quantify the differences between the two spectra, we applied a standard fitting procedure using four Gaussian-Lorentzian peak shapes (after subtraction of Al $K\alpha$ satellite contributions and a Shirley-type background). The intensity ratios between two pairs I_A/I_B and I_C/I_D are given in the figure for both spectra, clarifying the differences between them.

The valence-band spectrum was measured with HeI (21.2 eV) radiation, and the results are presented in Fig. 7, together with a representative spectrum of tenorite, taken by Ghijsen *et al.*[21] For the tenorite phase, the spectrum is representative to that obtained by other groups.[14,21–24] For example, there are no states at the Fermi level, which is as expected for an insulator.

Comparing the spectra for tenorite and our CuO, there are some notable differences. The peak at low binding energy (~1.9 eV), which is caused by both oxygen and copper orbitals,[25] is not as strong in our spectrum as it is in the spectra of tenorite. Also the largest peak, mainly belonging to copper, clearly consists of two separate peaks in the tetragonal CuO spectrum and is not observed before for tenorite. For a film of this thickness, we cannot entirely exclude some contribution of the substrate to the spectrum. $SrTiO_3$

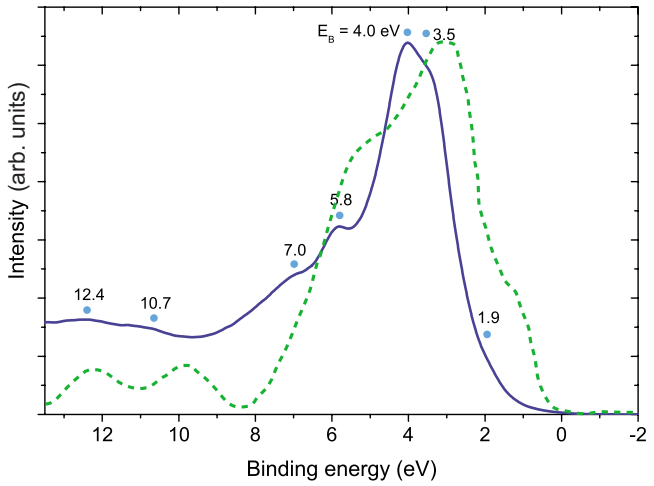

FIG. 7. (Color online) The tetragonal CuO valence-band spectrum (solid blue line) measured with HeI radiation and the peak positions indicated with cyan dots. The dotted line is a tenorite spectrum taken at 21.2 eV radiation by Ghijsen *et al.* (Ref. 21).

has two large oxygen peaks at about 4.4 and 6.6 eV as observed by Siemons *et al.*[26] Finally, two features at higher binding energy (>10 eV) are observed in both spectra.

VI. ELECTRONIC STRUCTURE: DISCUSSION

Comparison of our XPS results for the tetragonal form of CuO with those for tenorite reveals that (1) the main peak becomes broader, (2) the intensity distribution in the satellite peak shifts more to lower binding energies, and, finally, (3) the satellite peak intensity changes relative to that of the main peak when tetragonal phase is formed. (1) According to Van Veenendaal and Sawatzky,[27,28] the width of the main peak is related to whether the screening electrons come from the closest ligand atoms or from ligand atoms further away. This would suggest that the screening electrons are more delocalized in the tetragonal structure. Note that while the shortest Cu-O bond lengths in the tetragonal structure are similar to those in tenorite, there are also much longer bond lengths in the tetragonal structure, which might have an influence on the nature of the screening electrons. In our XPD simulations, we have assumed all 180° Cu-O-Cu bonds for the construction of the unit cell, whereas they could be less due to Jahn-Teller distortions, for example. Other measurements are required to accurately determine the bond angles, which are known to have a profound impact on especially the magnetic properties. A correlation between the width of the main peak and the oxygen coordination of Cu in a specific compound was suggested by Parmigiani *et al.*[29] Analysis of the XPS spectra on this basis would imply a higher oxygen coordination of Cu in the tetragonal phase.

(2) The structure of the satellite peak is harder to understand. The similarity with $CuCl_2$ spectra from the literature is striking though.[30] Okada and Kotani[31] performed extensive modeling of the satellite peak of $CuCl_2$. They argued that the shape of the satellite peak is mostly determined by the coupling-strength ratio between the σ and π bondings and the amount of hybridization of these states. Following their model suggests that the degree of hybridization is weaker in the tetragonal structure than in tenorite. In other words, the bonding in the tetragonal structure seems to have a more ionic character. A similar conclusion was reached by Böske *et al.*[32] for the compound $Sr_2CuO_2Cl_2$, which they compared to La_2CuO_4. More generally, comparing the Cu $2p$ structure to that of high-T_c compounds,[20,33] we find the structure of the satellite peak to be very similar, with more spectral weight at lower binding energy. For most compounds, a broadening of the main peak or the existence of a shoulder is also observed.[19] (3) A more quantitative comparison of the electronic structure of the Cu $2p$ peak structure with that other copper compounds is given in Table I.

From the numbers in the table, we conclude that tetragonal CuO compares to $CuCl_2$ in the copper halide series, whereas tenorite is closer to $CuBr_2$. For the $MCuO_4$ series, the values for tetragonal CuO are closest to Bi_2CuO_4. Following the analysis of Tranquada *et al.*,[34] where the authors

TABLE I. Intensity ratios between main peak and satellite as well as their energy separation. Note that the position of the peaks has been determined as the weighted average of the fitted components (see Fig. 6).

Compound	$I(\underline{2p}\ 3d^9)/I(\underline{2p}\ 3d^{10}\underline{L})\ (2p_{3/2})$	$E(\underline{2p}\ 3d^9)-E(\underline{2p}\ 3d^{10}\underline{L})\ (2p_{3/2})$ (eV)
CuO monoclinic	0.46	8.2
CuO tetragonal	0.58	7.7
CuO[a]	0.55	9
CuF_2 [b]	0.8	7
$CuCl_2$ [a]	0.6	8.8
$CuBr_2$ [a]	0.45	10
$Ca_{0.85}Sr_{0.15}CuO_2$ [c]	0.34	8.8
Nd_2CuO_4 [c]	0.35	9.0
La_2CuO_4 [c]	0.45	8.2
Bi_2CuO_4 [c]	0.62	8.2

[a]Reference 21.
[b]Reference 30.
[c]Reference 34.

found an empirical relationship between the position of the main peak and the intensity ratio between the satellite and main peak, we conclude that both tenorite [binding energy (BE) $Cu(2p_{3/2})=934$ eV] and tetragonal CuO [BE $Cu(2p_{3/2})=934.2$ eV] follow this trend. Therefore, also based on their accompanying cluster calculation, one can conclude that tetragonal CuO has a larger optical gap compared to tenorite (which resembles La_2CuO_4).

The UPS spectrum of tetragonal CuO is very similar to that measured for tenorite. Some notable differences include the intensity of the low-energy peak, the splitting of the main peak, and a general shift of the spectrum to higher binding energies of about half an eV. Delocalized band calculations (local-density approximation) performed for tenorite do not reproduce measurements on the tetragonal phase, suggesting the valence bands are changed with the structural change. Electron correlation effects are important in these materials and neglecting them results in incomplete density of states (DOS) spectra and conducting ground states. The best predictions come from cluster calculations [configuration-interaction (CI) calculations], which predict the entire spectrum accurately, but shifted to slightly lower binding energy. Note that calculations on the tenorite band structure show a splitting of this peak,[21,25] and in some measurements a shoulder is visible.[22] The peaks at 5.8 and 7.0 eV are both oxygen peaks and are also predicted by calculations.[25] The double peak feature at higher energy (10–13 eV) is a copper feature only predicted by the most advanced calculations.[23,25,35,36] All calculations on tenorite predict the peaks to be at lower binding energies than measured here, and the spectrum we observe is shifted up by as much as 2 eV. The spectrum for the tetragonal phase is shifted to higher binding energies by about 0.5 eV compared to the tenorite phase. Speculatively, assuming that the Fermi level is in the middle of the gap, this would imply a larger charge-transfer gap Δ. This is further supported by the broadening of the main peak of the Cu $2p$ doublet, which is expected theoretically[37] when Δ is increased. Eskes *et al.*[35] investigated the nature of the first ionization state of CuO, which has either a triplet or a singlet character. The singlet state peak is the one closest to the Fermi level (1.9 eV in our spectrum) and the triplet state is the next one up (3.6 eV for this work). The energy difference between these peaks is closely related to the Cu-O distances, specifically, the ratio between the Cu-O distance out of plane and in plane, which is about 1.4 for the tetragonal unit cell. Based on their model, we would expect to see an energy difference of 0.85 eV between the two peaks. The measured distance is much larger for reasons that are not well understood. An important next step in this research will be to specifically calculate the band structure for the tetragonal CuO.

VII. INITIAL DOPING EXPERIMENTS

As mentioned in the introduction, we have made some preliminary attempts to dope our new tetragonal form of CuO, which like the other transition metal monoxides, we expect it to be a Mott insulator of the charge-transfer type.[38,39] To attempt charge-transfer doping, without breaking vacuum, alkali metals were deposited on top of our tetragonal CuO films. Alkali metals were chosen because their outer electrons are very weakly bound and would be expected to be transferred into the CuO. This property also makes them very reactive, and so we have not attempted analyzing these samples outside our deposition chamber. Of course, even if charge is transferred the question remains whether the charges will be mobile or localized. A capability to measure the transport properties of our samples without leaving the UHV environment is under development.

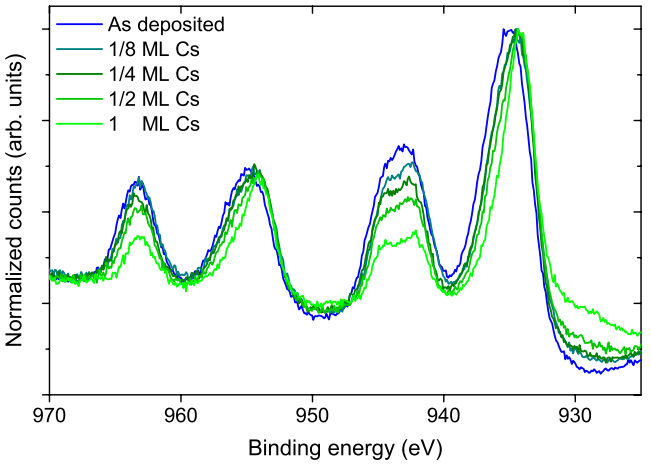

FIG. 8. (Color online) XPS Cu $2p$ spectrum of an as-deposited tetragonal CuO film and spectra taken after deposition of approximately $\frac{1}{8}$, $\frac{1}{4}$, $\frac{1}{2}$, and 1.0 MLs of Cs. The spectrum changes systematically toward a Cu^{1+} spectrum, which suggests charge carriers are created. The increase in the background at low binding energy is caused by a nearby Cs peak.

Two alkali metals were used: Li and Cs. The XPS results of one of the charge-transfer doping experiments using Cs are shown in Fig. 8. Deposition was incremental, and after each deposition photoemission spectra were taken. The Cu $2p$ spectra in Fig. 8 show a systematic change with increasing Cs coverage. The O $1s$ peak at about 530 eV does not change significantly when Cs is deposited (not shown). The Cs peaks themselves are at lower BE than one would expect for elemental Cs by about 1 eV. CsOH is 1.4 eV lower than Cs metal, and the lower binding energy, therefore, suggests that Cs has donated an electron. The spectral shift in the $2p$ peaks can be explained by doping of the Cs electrons into the CuO. In a localized picture, this would generate more Cu^{1+} at the expense of Cu^{2+} and make the spectrum look more like Cu_2O, which has been shown theoretically.[40] On the other hand, a similar effect would be expected to occur if Cs removed oxygen from the CuO, which also creates more Cu^{1+}. In both cases, the CuO would be electron doped. The decrease in the satellite peak as a function has also been seen in other compounds (see, for example, the review by Kohiki).[41] UPS measurements showed no Fermi edge, and some charging was observed during XPS measurements. Note that we used the Ti $2p$ peak from the substrate as an internal energy reference. The Li-doped samples showed a similar trend.

VIII. CONCLUSION

In conclusion, through the use of epitaxy, a nearly rocksalt form of CuO has been synthesized that is now available for physical study. The RHEED and XPD results seem unequivocal that a tetragonal structure of CuO has been synthesized through the use of epitaxy. The more interesting question is what are the electronic properties of this higher-symmetry phase. Preliminary electron structure studies and comparison with trends in known compounds in literature suggest that the charge-transfer gap Δ is enhanced in the tetragonal phase and the overall bonding seems more ionic. Note that this is a bit at odds with our current structural analysis, where a 180° bond angles were assumed; but one has to realize that this analysis was best effort for such ultrathin films, keeping all analysis under UHV conditions. As a new end member of the 3*d* transition monoxides, its magnetic properties should be that of a high T_N antiferromagnet.

ACKNOWLEDGMENTS

This work was supported by the Department of Energy with additional support from EPRI. We would like to thank P. M. Grant for many useful conversations and his continuing interest in this work. We would also like to acknowledge W. A. Harrison and G. A. Sawatzky for useful conversations and A. Vailionis for critical help in understanding the RHEED patterns.

*Corresponding author. gkoster@utwente.nl

[1] J. Bednorz and K. Muller, Rev. Mod. Phys. **60**, 585 (1988).
[2] L. F. Mattheiss, Phys. Rev. B **5**, 290 (1972).
[3] K. Terakura, T. Oguchi, A. R. Williams, and J. Kübler, Phys. Rev. B **30**, 4734 (1984).
[4] W. A. Harrison, Phys. Rev. B **76**, 054417 (2007).
[5] J. Zaanen and G. A. Sawatzky, Can. J. Phys. **65**, 1262 (1987).
[6] T. Kimura, Y. Sekio, H. Nakamura, T. Siegrist, and A. P. Ramirez, Nature Mater. **7**, 291 (2008).
[7] A. Georges, G. Kotliar, W. Krauth, and M. J. Rozenberg, Rev. Mod. Phys. **68**, 13 (1996).
[8] C. H. Ahn, J.-M. Triscone, and J. Mannhart, Nature (London) **424**, 1015 (2003).
[9] P. R. Willmott, R. Timm, P. Felder, and J. R. Huber, J. Appl. Phys. **76**, 2657 (1994).
[10] N. J. C. Ingle, R. H. Hammond, M. R. Beasley, and D. H. A. Blank, Appl. Phys. Lett. **75**, 4162 (1999).
[11] G. Koster, B. L. Kropman, G. J. H. M. Rijnders, D. H. A. Blank, and H. Rogalla, Appl. Phys. Lett. **73**, 2920 (1998).
[12] S. Spruytte, C. Coldren, J. Harris, D. Pantelidis, H.-J. Lee, J. Bravman, and M. Kelly, J. Vac. Sci. Technol. A **19**, 603 (2001).
[13] W. Siemons, Ph.D. thesis, University of Twente, 2008.
[14] Z.-X. Shen, R. S. List, D. S. Dessau, F. Parmigiani, A. J. Arko, R. Bartlett, B. O. Wells, I. Lindau, and W. E. Spicer, Phys. Rev. B **42**, 8081 (1990).
[15] N. Nakagawa, H. Hwang, and D. Muller, Nature Mater. **5**, 204 (2006).
[16] A. Catana, J.-P. Locquet, S. M. Paik, and I. K. Schuller, Phys. Rev. B **46**, 15477 (1992).
[17] F. J. García de Abajo, M. A. Van Hove, and C. S. Fadley, Phys. Rev. B **63**, 075404 (2001).
[18] Y. A. Teterin, M. I. Sosulnikov, and Y. A. Petrov, J. Electron Spectrosc. Relat. Phenom. **68**, 469 (1994).
[19] R. P. Vasquez, C. U. Jung, J. Y. Kim, M.-S. Park, H.-J. Kim, and S.-I. Lee, J. Phys.: Condens. Matter **13**, 7977 (2001).
[20] R. P. Vasquez, D. L. Novikov, A. J. Freeman, and M. P. Siegal, Phys. Rev. B **55**, 14623 (1997).
[21] J. Ghijsen, L. H. Tjeng, J. van Elp, H. Eskes, J. Westerink, G. A. Sawatzky, and M. T. Czyzyk, Phys. Rev. B **38**, 11322 (1988).
[22] W. Y. Ching, Y.-N. Xu, and K. W. Wong, Phys. Rev. B **40**, 7684 (1989).
[23] J. Ghijsen, L. H. Tjeng, H. Eskes, G. A. Sawatzky, and R. L. Johnson, Phys. Rev. B **42**, 2268 (1990).
[24] S. Warren, W. R. Flavell, A. G. Thomas, J. Hollingworth, P. L. Wincott, A. F. Prime, S. Downes, and C. Chen, J. Phys.: Condens. Matter **11**, 5021 (1999).
[25] M. Takahashi and J.-I. Igarashi, Phys. Rev. B **56**, 12818 (1997).
[26] W. Siemons, G. Koster, H. Yamamoto, T. H. Geballe, D. H. A. Blank, and M. R. Beasley, Phys. Rev. B **76**, 155111 (2007).
[27] M. A. van Veenendaal and G. A. Sawatzky, Phys. Rev. Lett. **70**, 2459 (1993).
[28] M. A. van Veenendaal, H. Eskes, and G. A. Sawatzky, Phys. Rev. B **47**, 11462 (1993).
[29] F. Parmigiani, L. E. Depero, T. Minerva, and J. B. Torrance, J. Electron Spectrosc. Relat. Phenom. **58**, 315 (1992).
[30] G. van der Laan, C. Westra, C. Haas, and G. A. Sawatzky, Phys. Rev. B **23**, 4369 (1981).
[31] K. Okada and A. Kotani, J. Phys. Soc. Jpn. **58**, 2578 (1989).
[32] T. Böske *et al.*, Phys. Rev. B **56**, 3438 (1997).
[33] P. Steiner, V. Kinsinger, I. Sander, B. Siegwart, S. Hüfner, and C. Politis, Z. Phys. B: Condens. Matter **67**, 19 (1987).
[34] J. M. Tranquada, S. M. Heald, W. Kunnmann, A. R. Moodenbaugh, S. L. Qiu, Y. Xu, and P. K. Davies, Phys. Rev. B **44**, 5176 (1991).
[35] H. Eskes, L. H. Tjeng, and G. A. Sawatzky, Phys. Rev. B **41**, 288 (1990).
[36] L. H. Tjeng *et al.*, Phys. Rev. Lett. **78**, 1126 (1997).
[37] K. Okada, A. Kotani, K. Maiti, and D. D. Sarma, J. Phys. Soc. Jpn. **65**, 1844 (1996).
[38] N. F. Mott, Proc. R. Soc. London, Ser. A **62**, 416 (1949).
[39] J. Zaanen, G. A. Sawatzky, and J. W. Allen, Phys. Rev. Lett. **55**, 418 (1985).
[40] K. Okada and A. Kotani, J. Phys. Soc. Jpn. **74**, 653 (2005).
[41] S. Kohiki, Spectrochim. Acta, Part B **54**, 123 (1999).